

Piezoelectric and ferroelectric properties of various amino acids and tubular dipeptide nanostructures: Molecular modelling

V. S. Bystrov^{1,*}, I. K. Bdikin² and Budhendra Singh^{2,3}

¹*Institute of Mathematical Problems of Biology, Keldysh Institute of Applied Mathematics, RAS, 142290 Pushchino, Moscow region, Russia*

**Corresponding author, e-mail address: vsbys@mail.ru*

²*TEMA-NRD, Mechanical Engineering Department and Aveiro Institute of Nanotechnology (AIN), University of Aveiro, 3810-193 Aveiro, Portugal*

³*Department of Physics, Central University of South Bihar, Gaya-Panchanpur Road, Gaya-824236, India*

Received 19 November 2019; accepted 20 February 2020; published online 10 March 2020

ABSTRACT

Piezoelectric and ferroelectric properties of dipeptide nanotubes (PNT) based on phenylalanine (F), alanine (A) and branched-chain amino acids (BCAAs) isoleucine (I), leucine (L) are investigated. Homodipeptides, such as di-isoleucine (II), di-leucine (LL), and heterodipeptides alanine-isoleucine (AI) dipeptides, and diphenylalanine (FF), are studied by molecular modeling using a quantum-mechanical (QM) semi-empirical PM3 method in a restricted Hartree-Fock (RHF) approximation based on the HyperChem package. After optimization of the models by the Polak-Ribiere conjugate gradient method, the total dipole moment and polarization of PNTs are calculated, with orientation along c-axis of a PNT with L-chiral isomer and alpha-helix conformation. The values obtained are: Pz (LL) ~ 3.6 $\mu\text{C}/\text{cm}^2$, Pz (II) ~ 6 $\mu\text{C}/\text{cm}^2$, Pz(AI) ~ 8.02 $\mu\text{C}/\text{cm}^2$, Pz(FF) ~ 2.3 $\mu\text{C}/\text{cm}^2$, which are comparable with the known data on the phenylalanine (FF) PNT polarization (for L-chiral in beta-conformation), which are of the order of Pz ~ 4 $\mu\text{C}/\text{cm}^2$. These polarizations allow us to calculate the piezoelectric coefficients d_{33} along the c-axis (in accordance with known electromechanical coupling relationship): 1) $d_{33}(\text{LL}) \sim 8 \text{ pm/V}$, $d_{33}(\text{II}) \sim 10 \text{ pm/V}$, $d_{33}(\text{AI}) \sim 26 \text{ pm/V}$, $d_{33}(\text{FF}) \sim 35 \text{ pm/V}$ (for $\epsilon = 4$); 2) $d_{33}(\text{LL}) \sim 12 \text{ pm/V}$, $d_{33}(\text{II}) \sim 15 \text{ pm/V}$, $d_{33}(\text{AI}) \sim 39 \text{ pm/V}$, $d_{33}(\text{FF}) \sim 52 \text{ pm/V}$ (for $\epsilon = 6$). These results are comparable with earlier data for FF PNT $d_{33}(\text{FF}) \sim 50 \text{ pm/V}$ (in beta-sheet conformation, L-chirality). The data obtained are confirmed by corresponding experimental AFM/PFM observations and measurements.

1. INTRODUCTION

All amino acids (AA) have their own dipole moments [1, 2], which interact with one another while amino acids or their dipeptides and polypeptides self-assemble into more complex molecular structures [3], such as molecular crystal structures (for example, based on the AA Glycine in various polymorphic forms [4-6]), various tubular structures, such as dipeptide nanotube (PNT) [7-12] and ion channel structures in biological

membranes [13 - 17]. Many of them are useful in materials science and medicine. It is established that many of these structures possess piezoelectric and ferroelectric properties [9-12, 18, 19]. Many similar organic structures having ferroelectric properties are considered now as organic ferroelectrics [19, 20]. Such structures based on AA, as well as on various DNA bases or other biological structures, demonstrating ferroelectricity (and piezoelectricity) are called bioferroelectrics (and biopiezoelectrics). They were intensively

studied by different methods, both experimentally and theoretically [6, 9-14]. As is well known, piezoelectricity usually arises as a result of electromechanical coupling in a given material [2, 12, 13]. This coupling is well known in biology – it can be observed in many biological processes: in a voltage-controlled muscle movement, in the nervous system, and in ion transport. [1, 13]. So this electromechanical coupling can be considered as the heart of ferroelectric and bioferroelectric phenomena.

A useful approach for such studies is computer molecular modeling, which allows one to calculate, investigate and predict the main physical properties of these structures based on AA. For example, diphenylalanine (FF) PNTs have been recently considered theoretically using molecular modeling by the quantum-chemical PM3 method (in HyperChem software) and experimentally using atomic force microscopy (AFM)/piezo-response force microscopy (PFM) measurements [9-12, 21-23].

But not only PNTs having aromatic (benzene) rings, such as FF, can demonstrate piezo/ferroelectric properties.

As pointed out by Leuchtag [13, 16], the branched-chain amino acids (BCAAs) Isoleucine (I), Leucine (L) and Valine (V), are known to exhibit ferroelectric properties with extremely large values of spontaneous polarization and dielectric permittivity [24, 25]. In the present work the piezoelectric and ferroelectric properties of the PNTs based on BCAA homodipeptides such as di-isoleucine (II), di-leucine (LL) and the heterodipeptide alanine-isoleucine (AI) are studied using molecular modeling by the PM3 method, and using experimental AFM/PFM measurements.

Here we deal only with α -helix conformations and L-chiral initial BCAAs molecules. D-chiral (the same as in a recent study [26]) and beta-sheet conformations (which were earlier used for FF PNT [9-12, 21-23]) will be considered later. It is known from experimental X-ray measurements that FF PNTs have the shape of an isolated ring with six dipeptides that form parallel stacking of two rings to form a crystal hexagonal structure [8] or two-layer rings in tubular models of these PNTs [11, 23]. However, for PNTs with BCAAs, only four dipeptides can form a similar isolated ring and construct a crystal structure [8, 27], as well as

similar tubular models of PNT[11, 23].

In this work we consider the structures and properties of several amino acids, their dipeptides and corresponding tubular nanostructures by molecular modeling using HyperChem package within the quantum-chemical semi-empirical PM3 approach in restricted Hartree-Fock (RHF) and unrestricted Hartree-Fock (UHF) approximations. The main results of computational data obtained for polarization and piezoelectric properties (piezoelectric coefficients d_{33}) are analysed in comparison with other known data and experimental observations.

2. COMPUTATIONAL DETAILS AND MAIN MODELS

In this work, the main tool used for the molecular modelling of all the studied nanostructures was the HyperChem 8.01 package [28]. Various computational methods were used, such as the molecular mechanics (MM) methods (including MM+, Amber, BIO CHARM), quantum mechanical (QM) self-consistent field (SCF) Hartree-Fock (HF) calculations, and semi-empirical methods (such as PM3, ZINDO-1), in the restricted Hartree-Fock (RHF) and unrestricted Hartree-Fock (UHF) approximations. The use of both the MM and QM methods for molecular modeling allowed us to obtain the minimum of the total energy or the potential energy surface (PES) of the systems being modelled. As a result, all the molecular systems investigated reached their optimal atomic configuration. The optimization of molecular systems and finding of their optimal geometry is performed in this work using the Polak–Ribere (conjugate gradient method) algorithm, which determines an optimized geometry at their minimum total energy point (using PES). These computational methods were used for detailed debugging, validation and testing of the models. But for final calculations of the optimized models, the PM3 in RHF approximations were used (since both UHF and RHF approximations show the same results for the studied systems).

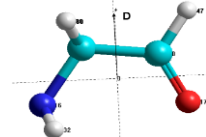
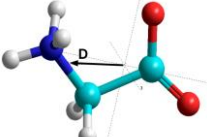
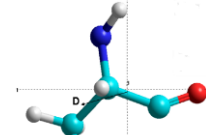
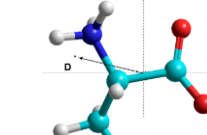
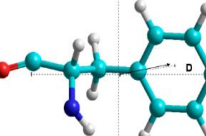
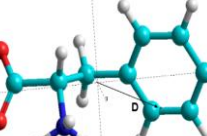
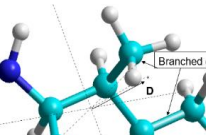
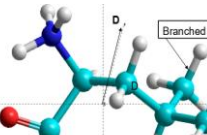
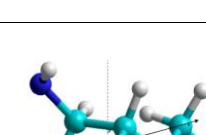
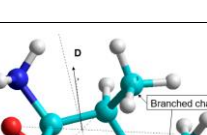
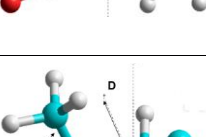
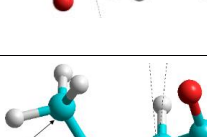
3. MAIN RESULTS AND DISCUSSIONS

First we investigate the initial amino acid properties. In HyperChem tool there is a special database for the main amino acids and we take it

for our modeling in HyperChem workspace. One of the important features is that all the amino acids (as well as dipeptides and polypeptides) exist in the initial pristine forms, but in all solutions (usually containing water) and in all reactions in living organism they exist in zwitterionic form. These forms can be created in HyperChem workspace

using a special option and we can work further with these zwitterionic structures. Another important feature is that all AA can exist in various conformations and chiralities (isomers). In this work we use alpha-helix conformation and L (left, from the Latin “laeva”) chirality.

Table 1. Several Amino Acid (AA) characteristics. (All atom colours are shown in the Fig.1 caption)

#	Amino Acid	Structure		I / ZW	D, Dipole moment, Debye	Polarization, C/m ²	Type
		I (initial pristine)	ZW (zwitterionic)				
1	Glycine (Gly, G)			I ZW	1.8 11.5	0.1 0.6	SC
2	Alanine (Ala, A)			I ZW	1.85 11.03	0.087 0.45	HSC
3	Phenylalanine (Phe, F)			I ZW	2.938 10.56	0.0676 0.2276	BSC
4	Leucine (Leu, L)			I ZW	2.763 10.013	0.0766 0.2562	BCAA
5	Iso-leucine (Ile, I)			I ZW	2.814 9.926	0.078 0.2538	BCAA
6	Valine (Val, V)			I ZW	1.396 9.973	0.045 0.292	BCAA

3.1. Dipole moments and polarizations of various amino acids

The possibility of a piezoelectric effect in various amino acids was indicated earlier by Lemanov [29, 30]. It should be noted that many of the amino acids considered by us have non-centrosymmetrical elements. This suggests a possibility of a piezoelectric effect in them. So, for example, valine, leucine, isoleucine have a symmetry group $P2_1$, and alanine and phenylalanine – $P2_12_12_1$ (while diphenylalanine exhibits hexagonal symmetry $P6_1$ [8]). In addition, like crystals based on glycine and diphenylalanine structures, these AAs have high polarizability, which is manifested when exposed to an electric field. This can be investigated using simulation methods which were described in [9-12, 31, 32].

Firstly we consider, the values of the dipole moment and polarization. Using the HyperChem tool and the database of amino acids we calculate

these values using RHF PM3 approach. As a result, we obtained data Table 1.

Abbreviations of AA Type in Table 1 are: Glycine – is a simplest special case (SC); all the other AA are the AA with Hydrophobic side chain (HSC): Alanine is the simplest of them; Phenylalanine is AA with an aromatic benzyl side chain (BSC); Leucine, Isoleucine and Valine are the branched-chain AA (BCAA).

As Table 1 shows, upon transition to the zwitterionic form, the dipole moment D increases significantly, which is not surprising, since in this ZW form the polar groups NH_3^+ and COO^- are more pronounced and are located at large distances from each other. The polarization value is:

$$P = 3.33556255 \cdot D/V \text{ (in C/m}^2\text{)},$$

where V is the structure's volume within the Van der Waals surface.

3.2. Di-peptides and Nanotubes of various AA

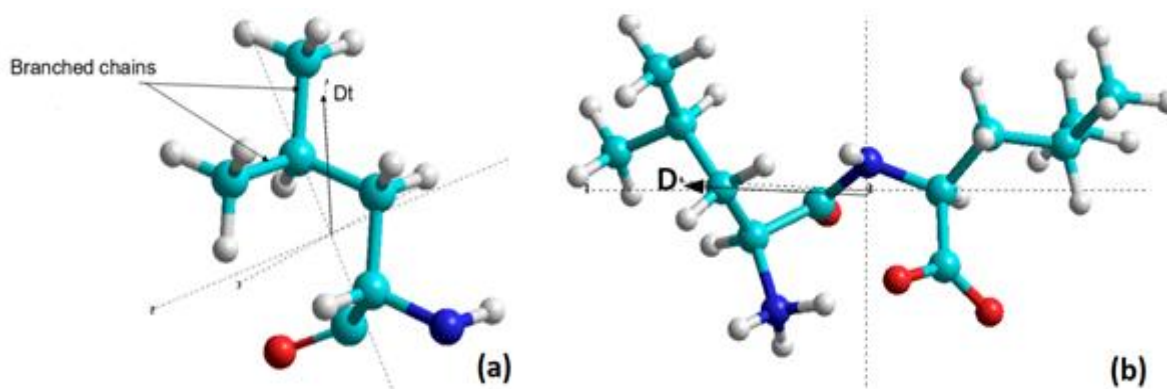


Figure 1. Structures based on the Leucine AA in ZW from: a) one molecule Leu, b) dipeptide Leu-Leu (LL). Atomic colour: Red – Oxygen, Deep Blue – Nitrogen, Cyan – Carbon, Gray – Hydrogen. The same for all atoms below too.

Table 2. Data calculated for Leucine AA structures.

Structure	Dipole, Debye	Polarization P, C/m ²	Dipole in ZW opt, Debye	Polarization P C/m ²	Dipole PNT Dt = ~ Dz, Debye	Volume of PNT, Å ³	Polarization P~Pz of PNT, C/m ²
Leu 1	2.763	0.077	10.013	0.2562			
di-leu			10.6194	0.14556			
4-di-leu in 1 ring					8.21	965.01	0.02838
2 rings di-leu					20.555	1928.27	0.03556

Next, we consider dipeptides primarily based on AA with the branched side chains (BCAA): namely, Leucine-Leucine (LL), Isoleucine-Isoleucine (II) and heterodipeptide, alanine-Isoleucine (AI).

3.2.1. Leucine (Leu or L) Leu-Leu or LL dipeptide

As we can see from the previous section (Table 1) - Leucine (Leu, or L) has its own initial dipole moment $D \approx -2.7$ Debye, in ZW form it is equal to $D \sim 10$ Debye.

Using the HyperChem tool we constructed a dipeptide in ZW form and calculated its properties

for a fixed atomic position (single point – SP – calculation). Then we performed PES optimization using the Polak–Ribere conjugate gradient method and obtained an optimized structure. The data obtained are presented in Fig. 1 and in Table 2 below.

After that we constructed 1 ring from 4 di-leucine (4-LL) and optimized it in a similar way. Finally, we designed a 2-ring peptide nanotube (PNT) model and optimized this structure. The results are presented in Fig 2,3 and the data computed are listed in Table 1, 2. Having compared the results obtained with experimental data [8] we can see that the shape of PNT is fully consistent

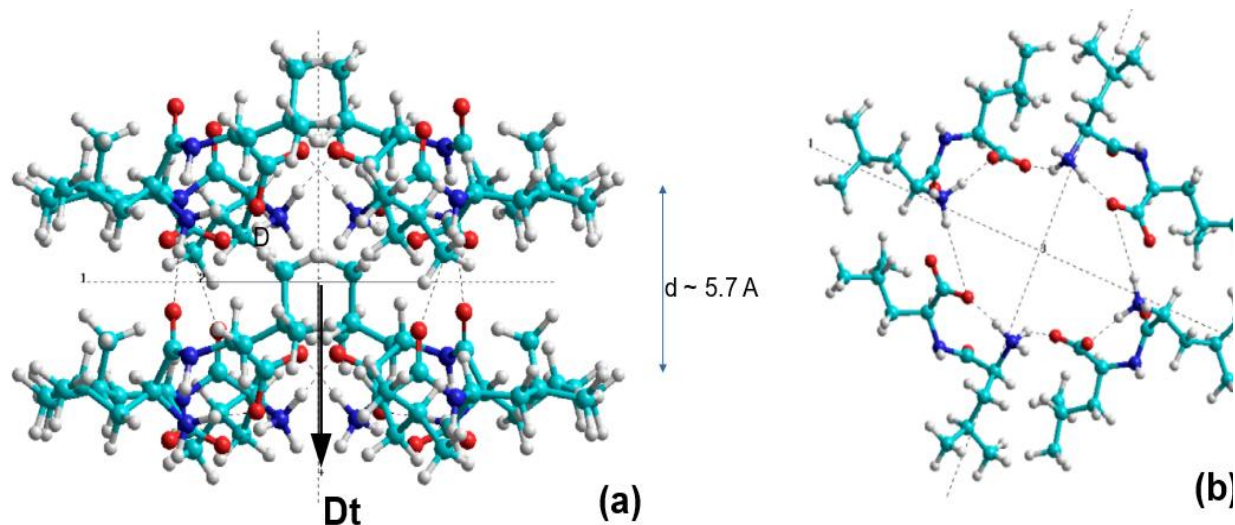


Figure 2. Tubular LL structures: a) side view (Y axis), b) top view (Z axis).

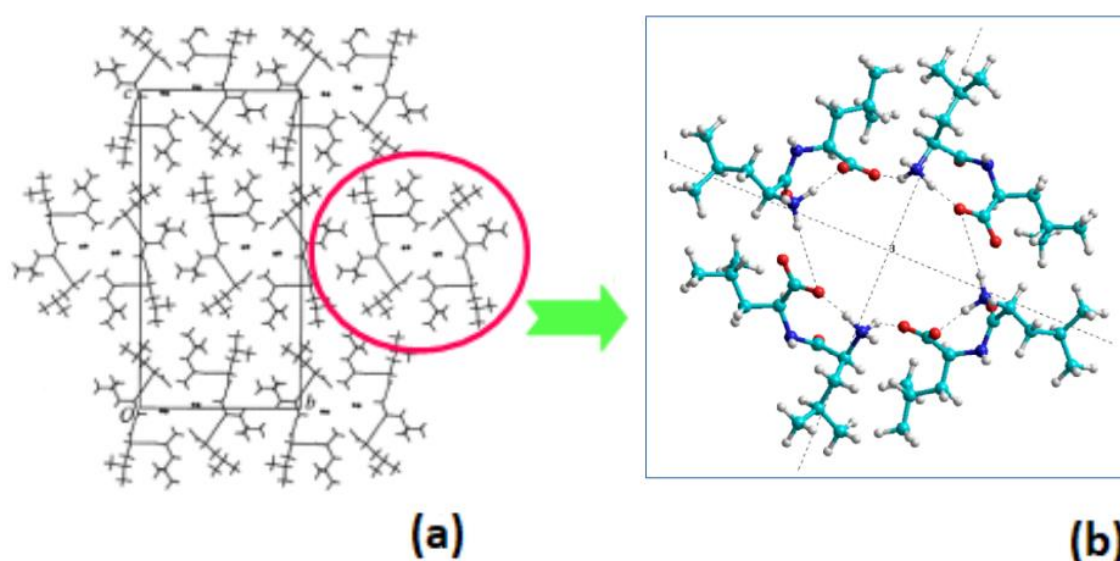


Figure 3. Comparison of LL PNT structure with experimental data from Gorbitz [8].

with the data obtained by X-ray. The experimental data for LL crystal orthorhombic unit cell are the following: $a = 5.3524 \text{ \AA}$, $b = 16.7600 \text{ \AA}$, $c = 33.312 \text{ \AA}$ (space group P212121). For our model, we have $a \sim 5.7 \text{ \AA}$ and the inner hollow width is approximately $\sim 8 \text{ \AA}$, which corresponds to doubled parameter b

$\sim 16 \text{ \AA}$.

3.2.2. Isoleucine (Ile or I) Ile-Ile or II dipeptide

For Isoleucine, the data obtained by similar calculations are presented below in Fig. 4,5 and Table 3.

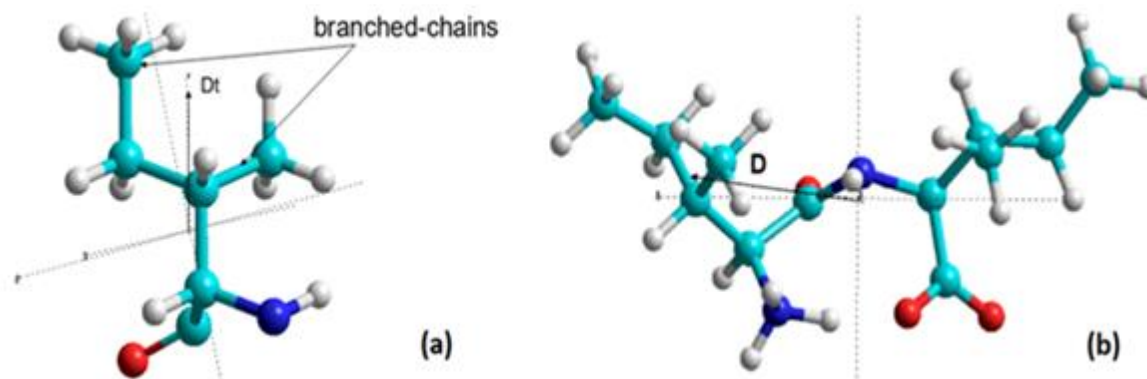


Figure 4. Structures based on Isoleucine AA in ZW form: a) one molecule Ile, b) dipeptide Ile-Ile (II)

Table 3. Data calculated for Isoleucine AA structures.

Structure	Dipole D, Debye	Polarization P, C/m ²	Dipole in ZW form, Debye	Polarization P in ZW, C/m ²	Dipole PNT Dt = ~ Dz, Debye	Volume of PNT, Å ³	Polarization P~Pz of PNT, C/m ²
Ile 1	2.814	0.078	9.926	0.2538			
di-Ile			11.7321	0.16064			
4-di-Ile 1 ring					16.7232	962.96	0.06017
2 rings di-Ile					35.180	1918.73	0.06116

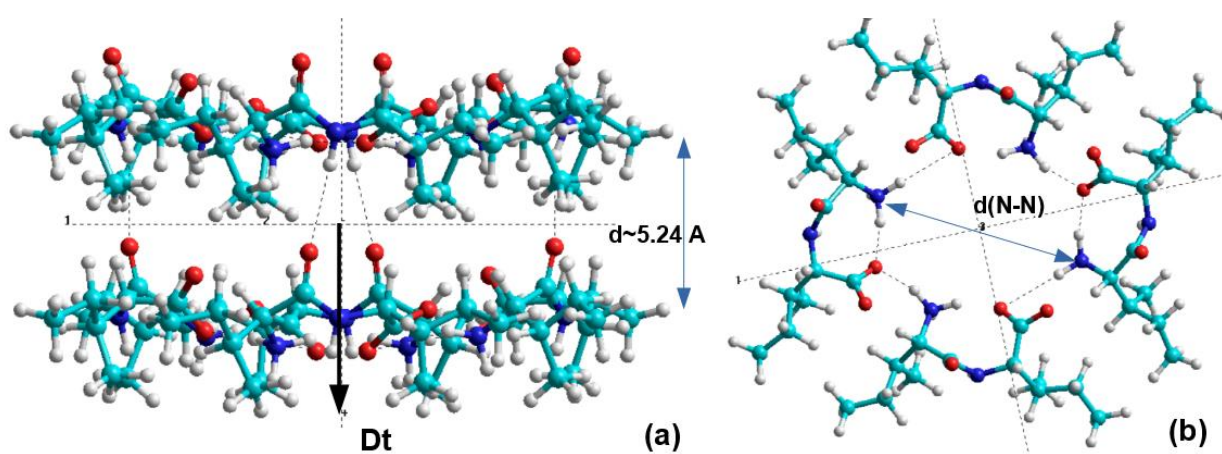


Figure 5. Tubular II structures: a) side view (Y axis), b) top view (Z axis); $d(\text{N-N}) \sim 8.0 - 8.5 \text{ \AA}$.

3.2.3. Alanine-Isoleucine (Ala-Ile) and AI dipeptide

For Alanine-Isoleucine combined structures similar calculations data obtained are presented below in Fig. 6, 7 and Table 4.

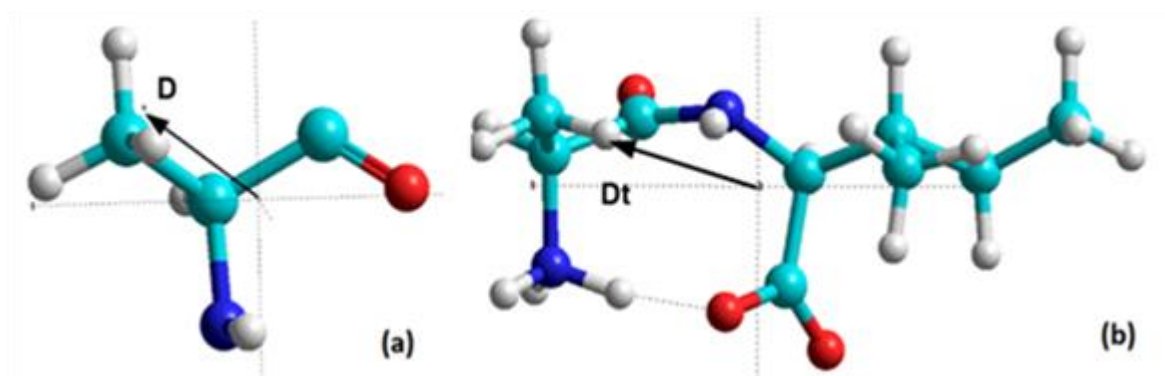


Figure 6. Structures based on the Alanine-Isoleucine AI in ZW form: a) one molecule Ala, b) dipeptide AI

Table 4. Data calculated for Alanine-Isoleucine AI structures.

Structure	Dipole D, Debye	Polarization P, C/m ²	Dipole in ZW form, Debye	Polarization P in ZW, C/m ²	Dipole PNT Dt = ~ Dz, Debye	Volume of PNT, Å ³	Polarization P~Pz of PNT, C/m ²
Ala 1	2.375	0.1113					
Ala-Ile			10.358	0.1782			
4-Ala-Ile 1 ring					15.0338	771.19	0.06502
2 rings Ala-Ile					36.869	1533.39	0.08020

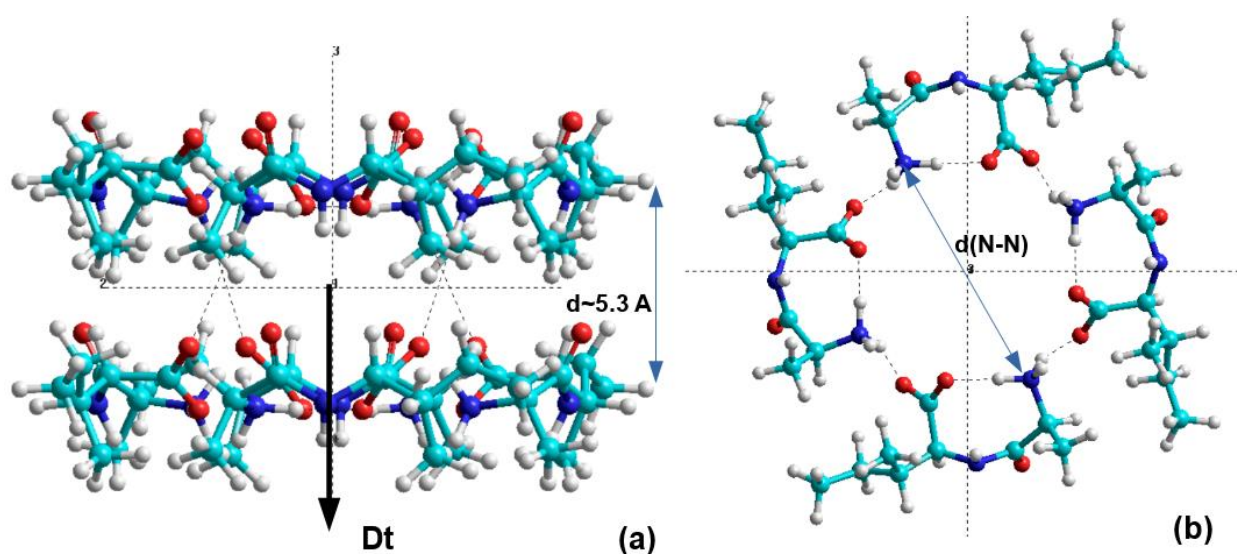


Figure 7. Tubular AI structures: a) side view (Y axis), b) top view (Z axis); average $d(N-N) \sim 8.1 \text{ \AA}$.

3.3. Piezoelectric coefficients calculations

In works [8, 27] the structures of AA crystals were studied, but the piezoelectric properties were not calculated. Now we can calculate the piezoelectric properties based on the common coupling of the local deformation of any materials in the electric field [2, 9-12].

Piezoelectricity is a phenomenon that can exist only in non-centrosymmetrical materials [2, 9]. The main building blocks of life are proteins, and the majority of protein crystals are non-centrosymmetrical. Proteins are made of combinations of 21 known amino acids [1], the majority of which also have the form of non-centrosymmetrical crystal structures. In the works by Lemanov *et al.* [29, 30] it was demonstrated that, as a consequence, these amino acids possess piezoelectric properties. He revealed the piezoelectric response of amino acid crystals, and attributed it to the rotation of the CH₃ and NH₃ groups [29, 30]. A similar common piezoelectric response is inherent in almost all organic and biological structures. Such biopiezoelectricity is exhibited in large-scale biological systems such as proteins, biopolymers, polysaccharides, organelles, and various organic piezoelectric biomaterials [9-20, 33-35].

As was already mentioned above, piezoelectricity arises from the electromechanical coupling in any given material [2, 9-12]. We can assume that biopiezoelectricity also arises from electromechanical coupling in bioorganic molecular nanostructures. The phenomenon is based on the known general relation between the piezoelectric constant d_{ik} , the electrostriction coefficient Q_{ik} , the permittivity of the material ϵ , the permittivity of vacuum $\epsilon_0 = 8.85 \cdot 10^{-12} \text{C}/(\text{Vm})$, and the component of polarization P_k of the whole system [2, 11, 36]. For a simple case, as a first approximation for only one component of the coefficient Q_{11} , the piezoelectric constant d_{33} , dielectric permittivity ϵ and spontaneous polarization P , the relationship can be written as [36, 37]:

$$d_{33} = 2Q_{11}\epsilon\epsilon_0P \quad (1)$$

On this basis, we can study piezoelectricity and

related changes in the dipole moments and polarization of various systems. We should only remember, that with such a local deformation of the material (or any molecular structure) under the influence of an electric field, in eq. (1), it is precisely the corresponding change in polarization, that must be taken into account. Therefore, the polarization P must be replaced by ΔP .

For example, using our data on the polarization of the computed AA (from Table 2, 3 and 4: $P(\text{LL}) \sim 0.036 \text{ C}/\text{m}^2$, $P(\text{II}) \sim 0.06 \text{ C}/\text{m}^2$, $P(\text{AI}) \sim 0.08 \text{ C}/\text{m}^2$) and the data obtained from the calculations for a similar structure FF PNT in our previous work [9-12] ($Q_{11} \sim 350 \text{ m}^4/\text{C}^2$, $\Delta P \sim 0.05P$ for the case of applied external electrical field along the main axis of PNT $E_z \sim 0.001 \text{ a.u.} \sim 5.14 \cdot 10^8 \text{ V}/\text{m}$), the values of piezoelectric coefficients for our tubular models of the investigated AA PNT (with $\epsilon = 4$ as in proteins) were estimated: $d_{33}(\text{LL}) \sim 44 \text{ pm}/\text{V}$, $d_{33}(\text{II}) \sim 73 \text{ pm}/\text{V}$, $d_{33}(\text{AI}) \sim 99 \text{ pm}/\text{V}$ [38]. These data are in good agreement with earlier obtained $d_{33}(\text{FF}) \sim 50 \text{ pm}/\text{V}$ for FF PNT [9-12].

However, we must take into account that such an estimate is very approximate and perhaps it gives overestimated values. Therefore, below we will conduct a more accurate and consistent calculation of such a local deformation of each of the studied tubular structures in the same electric field $E_z \sim 0.001 \text{ a.u.} \sim 5.14 \cdot 10^8 \text{ V}/\text{m}$, applied along the main OZ- axis of each AA PNT structure.

As usual, the value of the polarization P is obtained from the dipole moment D (in Debye units):

$$P = 3.33556255 \cdot D/V \quad (\text{in } \text{C}/\text{m}^2),$$

where V is the structure's volume on the Van der Waals surface.

3.3.1. Procedure of calculations

The molecular models of all the studied PNT were constructed using the database of amino acids (AA) from HyperChem tool [28]. All AA and relevant di-peptides were taken out in alpha helix conformation and in L chirality. (an exception was only for diphenylalanine, which was used besides alpha-helix, also in beta-sheet conformation for comparison with previous data [11, 12, 23, 26]).

First, after construction of the molecular models of any AA PNT, their structural optimization (by

Polak–Ribere conjugate gradient method) was performed to reach the most optimal nanostructure of AA PNT. All necessary parameters of these optimized AA PNT structures (such as dipole moment, volume, polarization, etc.) were calculated at this stage. These data are listed above in Table 2, 3 and 4.

Second, the electric field E_z along the main tubular axis of AA PNT was applied (using a special option in the HyperChem tool) and for the

optimized structure (with fixed positions of all the atoms) Single Point (SP) calculations were performed to obtain the changes of the dipole moment $\Delta D = D - D_0$ and polarization $\Delta P = P - P_0$ in this case. From these data, the value of electronic polarizability α for each PNT structure was estimated, relying on the fact that the deviation of the electric field ΔE_z is reckoned from $E=0$, $\Delta E_z = E_z$. These data of the polarizability $\alpha = \Delta D/E_z$ could be converted to atomic units (from

Table 5. Computed data for various AA PNT characteristics and parameters. (all the structures are in alpha-helix conformation and L-chirality, except for the last column with old L-FF data in beta-sheet conformation).

Parameter	L-Leu-Leu	L-Ile-Ile	L-Ala-Ile	L-FF-alpha [23, 26]	L-FF-beta [23]	L-FF-beta, old data [11,12]
$D_0=D_z$, Debye	20.56	35.18	36.87	23.89	38.29	42.70
$P_0=P_z$, C/m ²	0.036	0.061	0.080	0.023	0.037	0.041
$D(E_z=0.001 \text{ a.u.})$, fixed SP	18.37	32.98	35.09	19.54	33.19	37.45
$\Delta D=D-D_0$, Debye (in abs. value)	1.98	2.20	1.78	4.35	5.10	5.26
$\alpha=\Delta D/\Delta E$, Å ³	115.62	128.04	104.02	253.62	297.58	306
$\alpha=\Delta D/\Delta E$, a.u.	780.22	864.03	701.93	1711.54	2008.2	2068
D^{OPT} (opt. in $E_z=0.001 \text{ a.u.}$)	17.208	31.773	32.904	17.183	32.004	35.73
ΔD^{OPT} (opt. in E_z)	1.165	3.407	2.181	2.355	1.187	1.712
ΔP^{OPT} (opt. in E_z), C/m ²	0.002	0.006	0.005	0.002	0.001	0.002
$(\Delta P^{\text{OPT}})^2$, C ² /m ⁴	$4.06 \cdot 10^{-6}$	$3.513 \cdot 10^{-5}$	$2.25 \cdot 10^{-5}$	$5.102 \cdot 10^{-6}$	$1.3059 \cdot 10^{-6}$	$3.888 \cdot 10^{-6}$
V_0 , Å ³	1928.27	1918.73	1533.39	3477.59	3464.29	3503.17
$V(\text{opt})$, Å ³	1928.70	1917.27	1530.42	3481.49	3463.21	3498.42
$\Delta V=V-V_0$, Å ³	0.43	1.460	2.97	3.90	1.09	4.75
$S= \Delta V/V_0$	$2.23 \cdot 10^{-4}$	$7.62 \cdot 10^{-4}$	0.00194	0.00112	$3.1768 \cdot 10^{-4}$	0.0017
$Q=S/(\Delta P^{\text{OPT}})^2$, m ⁴ /C ²	54.95	21.68	77.26	219.64	243.20	348.80
$d=2\epsilon\epsilon_0 Q \Delta P^{\text{OPT}}$, ($\epsilon = 4$), pm/V	8.0	10.0	26.0	35.0	20.0	48.7~50.0
$d=2\epsilon\epsilon_0 Q \Delta P^{\text{OPT}}$, ($\epsilon = 6$), pm/V	12.0	15.0	39.0	52.5	30.0	73.0
$d=2\epsilon\epsilon_0 Q \Delta P^{\text{OPT}}$, ($\epsilon = 10$), pm/V	20.0	25.0	65.0	87.5	50.0	121.8

Debye unit for D) using the coefficient 1 Debye = 0.393456 a.u., with $E_z = 0.001$ a.u. The presentation of α in angstrom (\AA) unit can be made by dividing into the coefficient 6.74833: $\alpha(\text{\AA}^3) = \alpha(\text{a.u.})/6.74833$.

Thrid, the structural optimization (using again Polak–Ribere conjugate gradient method) under applied electric field E_z was carried out to reach a new optimal structure under the influence of this applied electric field. After this optimization all the atoms of PNT structures changed their positions and the total volume of the structures was changed to $-\Delta V = V - V_0$. For these new optimized PNT structures, all necessary calculations were performed again to obtain new changed data for dipole moments D^{OPT} (and $\Delta D^{\text{OPT}} = D^{\text{OPT}} - D$ in E_z), volume V and polarization P^{OPT} (and $\Delta P^{\text{OPT}} = P^{\text{OPT}} - P$ in E_z). As a result, the electrostriction and piezoelectric coefficients were calculated from these data obtained.

Electrostriction coefficient is determined by relation $Q_{11} = Q = S/(\Delta P^{\text{OPT}})^2$, where $S = \Delta V/V_0$.

Piezoelectric coefficient is finally calculated from the relation $d_{33} = d = 2\epsilon\epsilon_0 Q \Delta P^{\text{OPT}}$.

All the data, computed step by step using this procedure algorithm, are presented in Table 5.

Table 5 lists the data not only for AA PNT (LL PNT, II PNT and AI PNT) computed in this work, but also the data obtained from our previous works on FF PNT (last columns). The last data are also compared with our older calculations of FF PNT in beta-sheet conformation. As one can see, these data are slightly overestimated as compared to our earlier results due to a greater value of the volume deformation and electrostriction coefficient calculation. As a result, the value of the piezoelectric coefficient has a greater value too as compared to our present result. The reason is probably that due to some details of optimization of the models, which improved the initial structures, we followed a different PES optimization trajectory and got to a different PES minimum point.

In Table 5 several various values of dielectric permittivity ϵ ($= 4, = 6, = 10$) are used. Usually for proteins the value $\epsilon = 4$ is used, but in some cases it is not correct. Permittivity can change, especially in the case, when temperature is changed –

probably various conditions and permittivity can rise up and may be much greater than $\epsilon = 10$ [11–17, 24, 25]. Especially in the case, for example, of the dielectric anomaly of squid axon membrane near heat-block temperature which is close to the ferroelectric Curie-Weiss law, described by Leuchtag [17] and analysed by Bystrov in [11]. However, now we cannot determine these changes exactly either. Using these computed data for various permittivity values we can estimate only approximately the possible effect.

3.3.2. Discussion of piezoelectric phenomena in AA PNT

To analyse the data obtained we must first remark that all the AA PNT structures investigated are based on the long-range electrostatic interaction (following from dipole-dipole interactions of their molecular components) and including Van der Waals interactions involving the hydrogen-bonds, inherent to these structures with NH_3 , CH_3 and COO sides, especially in their zwitterionic form including water molecules. Using HyperChem tool it is easy to see how the hydrogen-bonding formation process proceeds (with direct visualization of all the molecular structures on the work-space of the monitor display screen), and how it changes during the optimization processes.

Thus, here we can see how exactly the dipole-dipole and Van der Waals interactions occur, how hydrogen bonds form, change, and affect the whole self-organization of the molecular system. The piezoelectric phenomena in similar structures are now in the focus of interest of many scientists. An example is provided by recently published papers on Piezoelectric Effects of Applied Electric Fields on Hydrogen-Bond Interactions [34], Piezoelectric Hydrogen Bonding [33] and on Role of Molecular Polarizability in Designing Organic Piezoelectric Materials [35].

Note here that the polarizability values and the electrostriction coefficients obtained in our calculations are close to data for many similar molecular structures [33 – 36, 39–41].

The most interesting is that the values of the piezoelectric coefficients obtained for various AA PNTs in our calculations are in line with the data for several hydrogen bonding systems. For example, the largest piezo-coefficient of 23 pm/V is found for

the aniline–nitrobenzene dimer, followed by 2-methyl-4-nitroaniline with 15 pm/V, and phenol-nitrobenzene with 12 pm/V [33]. The piezo-coefficient of the thiophenol-nitrobenzene (SPH-NBz) dimer computed in [34] was found to be 24.9 pm/V, greater than that of 2-methyl-4-nitroaniline (14 pm/V), the organic crystal with the largest known piezoelectric response. In [34] a mention was made that a linear correlation between piezo-coefficient and dipole moment/polarizability was established, suggesting that the dipole moment and polarizability of H-bonded systems should be considered carefully while designing new high level piezo-materials. The study of various forms of this SPH-Nbz in [34] showed that the estimated piezo-coefficients for the symmetric and anti-symmetric SPH-NBz tetramer units were found to be 20.90 pm/V and 22.20 pm/V, respectively. These values are very close to that of the SPH-NBz dimer. The authors of [34] wrote that not only the force constant and dipole moment but also the molecular polarizability of the H-bonded systems plays a crucial role in higher piezo- response. This conclusion is in full agreement with our results too and is encouraging. Therefore the data obtained confirm that many more similar H-bonded and AA tubular systems could be found with high piezo-response due to the ubiquity of hydrogen bonds in chemistry, materials and biological systems.

3.3.3. About Experimental observations of piezo-response in various AA PNT

New dipeptide nanotubes: Di-Leucine (LL), Alanine-Isoleucine (Ala-Ile, AI) and Di-Phenylalanine (Phe-Phe, FF) peptide nanotubes (PNTs) were grown and investigated. First experimental local measurement of piezoresponse parameters of LL, II, AI and FF PNTs were carried out (and will be reported in a separate paper).

The surface morphology of the material was visualized using microscope Hitachi, TM4000Plus, field-emission scanning electron microscopy with a field emission filament operating at 5-15 kV. Atomic Force Microscopy (AFM) measurements were carried out using a Veeco AFM Multimode Nanoscope (IV) MMAFM-2, Veeco microscopy. Local piezoelectric properties of the PNTs were visualized simultaneously by using Atomic Force Microscopy (AFM) in contact mode and

piezoresponse force microscopy (PFM) methods [42]. First experimental local measurement piezoresponse parameters of LL, II, AI and FF nanotubes and microcrystals are presented and analysed in comparison with modelled and computed data in [43].

4. CONCLUSIONS

In this work computational molecular modeling and quantum-chemical calculations were performed for several AA tubular structures using HyperChem tool. The systems investigated were: Leucine-Leucine (LL), Isoleucine-Isoleucine (II), Alanine-Isoleucine (AI) and Di-Phenylalanine (FF) molecular tubular structures – peptide nanotubes (PNT), which are part of the corresponding molecular crystals with a special symmetry space group and crystallographic system. The formation of these PNT proceeds as a self-assembly processes due to electrostatic dipole-dipole interaction and Van der Waals interaction with participation and reorganization of the hydrogen bonds net.

Using HyperChem tool it is possible to observe how the hydrogen-bonding formation process proceeds (with direct visualization of all the molecular structures on the work-space of the monitor display screen), and how it changes during the optimization processes. Therefore, here we can visually see how the dipole-dipole and Van der Waals interactions occur exactly, how hydrogen bonds form, change, and affect the whole self-organization of the molecular system.

The data obtained for several new self-assembled PNTs (with AA in alpha-helix conformation and L-chiral isomer) are the following:

- 1) Average polarization:
 $P(\text{LL}) = 0.036 \text{ C/m}^2$, $P(\text{II}) = 0.061 \text{ C/m}^2$, $P(\text{AI}) = 0.0802 \text{ C/m}^2$, $P(\text{FF}) = 0.023 \text{ C/m}^2$;
- 2) Piezoelectric coefficient:
 for $\varepsilon = 4$: $d_{33}(\text{LL}) = 8.0 \text{ pm/V}$, $d_{33}(\text{II}) = 10.0 \text{ pm/V}$,
 $d_{33}(\text{AI}) = 26.0 \text{ pm/V}$, $d_{33}(\text{FF}) = 35.0 \text{ pm/V}$;
 for $\varepsilon = 6$: $d_{33}(\text{LL}) = 12.0 \text{ pm/V}$, $d_{33}(\text{II}) = 15.0 \text{ pm/V}$,
 $d_{33}(\text{AI}) = 39.0 \text{ pm/V}$, $d_{33}(\text{FF}) = 52.5 \text{ pm/V}$;

These new data obtained are in line and comparable with other known values for similar molecular systems and are very important for

further investigations and practical applications.

In parallel we carried out experimental studies of these AA PNTs having prepared their samples by direct chemical synthesis and observation/measurement of surface topography and piezo-response using atomic force and piezo-response force microscopy (AFM/PFM). The data obtained by these experimental techniques confirm the computational results and demonstrate relative differences in piezo-responses of various AA PNTs. These experimental data are presented in a separate publication.

As a result, modeling and studies of various AA PNTs with electromechanical hydrogen bonds suggest that electrostatic dipole-dipole and Van der Waals interacting molecular structures will probably be ubiquitous and can be easily extended to other similar self-organizing molecular systems, using accurate quantum-chemical computational methods both semi-empirical and first-principles electronic structure calculations.

On the basis of the performed modeling and calculations (based on the self-consistent quantum-chemical calculations of the electron subsystem and taking into account electrostatic dipole-dipole interaction), we can conclude that electric-field driven molecular conformational changes in such and other similar self-assembled molecular structures will give a more substantial piezoelectric response and that deformable hydrogen bonds can be used to produce polar, self-assembled piezoelectric materials with novel desirable properties designed through computational approaches.

Thus, this work shows us an appropriate direction for further research and opens up new horizons for the analysis of these and related molecular systems, their modeling, calculations, prediction of their properties and the creation of new materials based on them.

ACKNOWLEDGMENTS

The authors are greatly thankful to Prof. Richard Leuchtag for great support, interest in this study and useful discussions, to the Russian Foundation for Basic Researches (RFBR): # 19-01-00519 A for partial support and the Portuguese Foundation for Science and Technology (FCT) for financial support: IF/00582/2015, BI (DOUTOR)/6323/2018).

REFERENCES

- [1] A. L. Lehninger, *Biochemistry. The Molecular Basis of Cell Structure and Function*. New York: Worth Publishers, Inc. (1972).
- [2] M. E. Lines and A. M. Glass, *Principles and Applications of Ferroelectrics and Related Materials*. Oxford: Clarendon Press (1977).
- [3] A. C. Mendes, E. T. Baran, R. L. Reis, H. S. Azevedo. Self-assembly in nature: using the principles of nature to create complex nanobiomaterials. *Wiley Interdiscip. Rev. Nanomed. Nanobiotechnol.* **5(6)**, 582–612 (2013).
- [4] Y. Iitaka, The crystal structure of β -glycine. *Acta Crystallogr.* **13**, 35–45 (1960); Y. Iitaka, The crystal structure of γ -glycine. *Acta Crystallogr.* **14**, 1–10 (1961).
- [5] E. Seyedhosseini, M. Ivanov, V. Bystrov, I. Bdikin, P. Zelenovsky, V. Ya. Shur, A. Kudryavtsev, E.D. Mishina, A. S. Sigov, A. L. Kholkin. Growth and Nonlinear Optical Properties of Glycine Crystals Grown on Pt Substrates. *Crystal Growth & Design*. **14(6)**, 2831-2837 (2014).
- [6] V.S. Bystrov, E. Seyedhosseini, I.K. Bdikin, S. Kopyl, A.L. Kholkin, S.G. Vasilev, P.S. Zelenovskiy, D.S. Vasileva & V.Ya. Shur. Glycine nanostructures and domains in betaglycine: Computational modeling and PFM observations. *Ferroelectrics*. **496**, 28–45 (2016).
- [7] M. R. Ghadiri, J. R. Granja, R. A. Milligan, D. E. McRee, N. Hazanovich N. Self assembling organic nanotubes based on cyclic peptide architecture. *Nature*. **366**, 324–327 (1993).
- [8] C. H. Görbitz. Nanotube formation by hydrophobic dipeptides. *Chem. Eur. J.* **7**, 5153–5159 (2001).
- [9] V. S. Bystrov, I. Bdikin, A. Heredia, R. C. Pullar, E. Mishina, A. Sigov and A. L. Kholkin, Piezoelectric nanomaterials for biomedical applications: piezoelectricity and ferroelectricity in biomaterials: from proteins to self-assembled peptide nanotubes. In: G. Ciofani and A. Menciassi, eds. *Piezoelectric nanomaterials for biomedical applications.. Berlin Heidelberg, Springer-Verlag*. 187-212 (2012).
- [10] V. S. Bystrov, E. Seyedhosseini, S. Kopyl, I. K. Bdikin, and A. L. Kholkin. Piezoelectricity and ferroelectricity in biomaterials: Molecular modeling and piezoresponse force microscopy measurements. *J. Appl. Phys.* **116(6)**, 066803 (2014).
- [11] V. S. Bystrov. Computer Simulation Nanostructures: Bioferroelectric Peptide Nanotubes. Bioferroelectricity: Peptide Nanotubes. Saarbruecken: LAP Lambert Academic Publishing. *OmniScriptum GmbH & Co. KG*. (2016).
- [12] V. S. Bystrov, E. Paramonova, I. Bdikin, S. Kopyl, A. Heredia, R. Pullar, A. Kholkin. BioFerroelectricity: Diphenylalanine Peptide Nanotubes Computational Modeling and Ferroelectric Properties at the Nanoscale. *Ferroelectrics*, **440 (01)**, 3 – 24 (2012).
- [13] H. R. Leuchtag, Voltage-Sensitive Ion Channels: Biophysics of Molecular Excitability, *Dordrecht: Springer* (2008).

- [14] H. R. Leuchtag and V. S. Bystrov, Theoretical models of conformational transitions and ion conduction in voltage-dependent ion channels: Bioferroelectricity and superionic conduction. *Ferroelectrics*, **220** (3-4), 157-204 (1999).
- [15] V. S. Bystrov, H. R. Leuchtag, Bioferroelectricity: Modeling the transitions of the sodium channel. *Ferroelectrics*, **155**, 19-24 (1994).
- [16] H. R. Leuchtag, Bioferroelectricity in models of voltage-dependent ion channels. *Ferroelectrics*, **236**, 23-33 (2000).
- [17] H. R. Leuchtag, Fit of the dielectric anomaly of squid axon membrane near heat-block temperature to the ferroelectric Curie-Weiss law, *Biophys. Chem.*, **53**, 197-205 (1995).
- [18] B. Coste, B. Xiao, J. S. Santos, R. Syeda, J. Grandl, K. S. Spencer, S. E. Kim, M. Schmidt, J. Mathur, A. E. Dubin, M. Montal, and A. Patapoutian, "Piezo proteins are pore-forming subunits of mechanically activated channels. *Nature*. **483**(7388), 176 (2012).
- [19] S. E. Kim, B. Coste, A. Chadha, B. Cook, and A. Patapoutian, The role of Drosophila Piezo in mechanical nociception. *Nature*. **483**, 209 (2012).
- [20] S. Horiuchi, R. Kumai and Y. Tokura, Hydrogen-bonding molecular chains for high-temperature ferroelectricity. *Adv. Mater.* **23**, 2098 (2011).
- [21] A. Heredia, I. Bdikin, S. Kopyl, E. Mishina, S. Semin, A. Sigov, K. German, V. Bystrov, A. L. Kholkin. Temperature-driven phase transformation in self-assembled diphenylalanine peptide nanotubes. Fast Track Communication. *J. Phys. D: Appl. Phys.* **43**, 462001 (2010).
- [22] I. Bdikin, V. Bystrov, I. Delgadillo, J. Gracio, S. Kopyl, M. Wojtas, E. Mishina, A. Sigov and A. L. Kholkin. Polarization switching and patterning in self-assembled peptide tubular structures. *J. Appl. Phys.* **111**, 074104 (2012).
- [23] V. S. Bystrov, S. A. Kopyl, P. Zelenovskiy, O. A. Zhulyabina, V. A. Tverdislov, F. Salehli, N. E. Ghermani, V. Ya. Shur & A. L. Kholkin. Investigation of physical properties of diphenylalanine peptide nanotubes having different chiralities and embedded water molecules. *Ferroelectrics*, **525**, 168-177 (2018).
- [24] K. Yoshino, T. Sakurai. Ferroelectric liquid crystals and their chemical and electrical properties. In: Goodby, J.W. et al, editors. *Ferroelectric Liquid Crystals: Principles, Properties and Applications*. Gordon and Breach: Philadelphia, 317-363 (1991).
- [25] A. Chen, C.- D. Poon, T. Dingemans, and E. T. Samulski. Ferroelectric liquid crystals derived from isoleucine. II. Orientational ordering by carbon-13 separated local field spectroscopy. *Liquid Crystals*. **24**, 255-262 (1998).
- [26] V. S. Bystrov, P. S. Zelenovskiy, A. S. Nuraeva, S. Kopyl, O. A. Zhulyabina, V. A. Tverdislov. Molecular modeling and computational study of the chiral-dependent structures and properties of the self-assembling diphenylalanine peptide nanotubes. *J. Mol. Mod.* **25**, 199 (2019).
- [27] C. H. Gorbitz. Hydrophobic dipeptides: the final piece in the puzzle. *Acta Cryst.*, **B74**, 311- 318 (2018).
- [28] HyperChem: Tools for Molecular modeling (release 8). Gainesville: Hypercube, Inc. (2002).
- [29] V. V. Lemanov, S. N. Popov, G. A. Pankova, Piezoelectric properties of crystals of some protein aminoacids and their related compounds, *Phys. Sol. Stat.*, **44**, 1929-1935 (2002).
- [30] V. V. Lemanov, S. N. Popov, G. A. Pankova, Protein amino acid crystals: Structure, symmetry, physical properties, *Ferroelectrics*. **285**, 581-590 (2003).
- [31] V. S. Bystrov, E. Seyedhosseini, I. Bdikin, S. Kopyl, S. M. Neumayer, J. Coutinho, A. Kholkin, BioFerroelectricity: Glycine and Thymine nanostructures computational modeling and ferroelectric properties at the nanoscale. *Ferroelectrics*. **475**(1), 107-126 (2015).
- [32] V. S. Bystrov. Photo-Ferroelectricity in diphenylalanine peptide nanotube. *Computational Condensed Matter*. **14**, 94-100 (2018).
- [33] K. A. Werling, M. Griffin, G. R. Hutchison and D. S. Lambrecht, Piezoelectric Hydrogen Bonding: Computational Screening for a Design Rationale. *J. Phys. Chem. A*. **118**, 7404-7410 (2014).
- [34] K. A. Werling, G. R. Hutchison, D. S. Lambrecht, Piezoelectric Effects of Applied Electric Fields on Hydrogen-Bond Interactions: First-Principles Electronic Structure Investigation of Weak Electrostatic Interactions. *J. Phys. Chem. Lett.* **4**(9), 1365-1370 (2013).
- [35] A. A. Gagrai, V. R. Mundlapati, D. K. Sahoo, H. Satapathy, and H. S. Biswal. The Role of Molecular Polarizability in Designing Organic Piezoelectric Materials. *Chemistry Select.* **1**, 4326 - 4331 (2016).
- [36] R. E. Newnham, V. Sundar, R. Yimnirun, J. Su, Q. M. Zhang, Electrostriction: Nonlinear Electromechanical Coupling in Solid Dielectrics. *J. Phys Chem B*. **101**, 10141-10150 (1997).
- [37] A. L. Kholkin, K. G. Brooks and N. Setter, Electromechanical properties of SrBi₂Ta₂O₉ thin films, *Appl. Phys. Lett.*, **71**(14), 2044 (1997).
- [38] V. S. Bystrov, I. K. Bdikin and Budhendra Singh, Piezoelectric and ferroelectric properties of various amino acids and dipeptides structures: molecular modeling and experiments. In: I. Bdikin, Budhendra Singh, Raul Simões, eds. 2nd International Conference on Nanomaterials Science and Mechanical Engineering. *Book of Abstracts. Aveiro, UA Editora, Universidade de Aveiro*, **44** (2019).
- [39] K. Yamada, A. Saiki, H. Sakae, S. Shingubara, and T. Takahagi, Study of a dielectric constant due to electronic polarization using a semiempirical molecular orbital method. *Jpn. J. Appl. Phys.* **40**, 4829-4836 (2001).
- [40] V. S. Bystrov, et al. Molecular modelling of the piezoelectric effect in the ferroelectric polymer poly(vinylidene fluoride) (PVDF). *J. Mol. Mod.*, **19**, 3591-3602 (2013).
- [41] V. S. Bystrov, Piezoelectricity in the ordered monoclinic hydroxyapatite. *Ferroelectrics*, **475**, iss.1, 148-153 (2015).

- [42] A. Roelofs, T. Schneller, K. Szot, R. Waser. Piezoresponse force microscopy of lead titanate nanograins possibly reaching the limit of ferroelectricity. [*Applied Physics Letters*, **81** \(27\), 5231-5233 \(2002\).](#)
- [43] Budhendra Singh, V. S. Bystrov, Nuno Almeida, I.K. BdiKin, Local piezoelectric properties of Di-Leucine and Alanine-Isoleucine dipeptides nanotubes. - in print.